AD-A159 028 EXTENSIONS OF THE FIELD EMISSION FLUCTUATION METHOD FOR THE DETERMINATION OF SURFACE DIFFUSION COEFFICIENTS(U) CHICAGO UNIV IL JAMES FRANCK INST R GOMER JUL 85 1/1

UNCLASSIFIED N00014-77-C-0018 F/G 7/4 NL

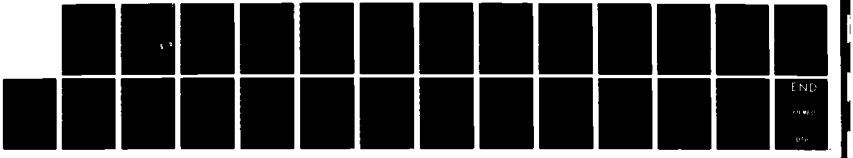

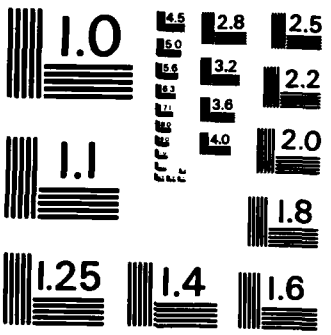

REPORT DOCUMENTATION PAGE

READ INSTRUCTIONS BEFORE COMPLETING FORM

1. REPORT NUMBER

2. GOVT ACCESSION NO.

3. RECIPIENT'S CATALOG NUMBER

4. TITLE (and Subtitle)
Extensions of the Field Emission Fluctuation Method for the Determination of Surface Diffusion Coefficients

5. TYPE OF REPORT & PERIOD COVERED

6. PERFORMING ORG. REPORT NUMBER

7. AUTHOR(s)
Robert Gomer

8. CONTRACT OR GRANT NUMBER(s)
N00014-77-C-0018

9. PERFORMING ORGANIZATION NAME AND ADDRESS
The University of Chicago
The James Franck Institute
5640 South Ellis Avenue, Chicago, Illinois 60637

10. PROGRAM ELEMENT, PROJECT, TASK AREA & WORK UNIT NUMBERS

11. CONTROLLING OFFICE NAME AND ADDRESS
Office of Naval Research
Physical Sciences Division
800 North Quincy St., Arlington, VA 22217

12. REPORT DATE
July 1985

13. NUMBER OF PAGES
23

14. MONITORING AGENCY NAME & ADDRESS(if different from Controlling Office)

15. SECURITY CLASS. (of this report)
unclassified

15a. DECLASSIFICATION/DOWNGRADING SCHEDULE

16. DISTRIBUTION STATEMENT (of this Report)

This document has been approved for public release and sale; its distribution is unlimited.

17. DISTRIBUTION STATEMENT (of the abstract entered in Block 20, if different from Report)

18. SUPPLEMENTARY NOTES
Prepared for publication in Applied Physics

19. KEY WORDS (Continue on reverse side if necessary and identify by block number)
Scanning Tunneling Microscopy
Surface Diffusion

20. ABSTRACT (Continue on reverse side if necessary and identify by block number)

The use of scanning tunneling microscopy and related techniques for the determination of surface diffusion coefficients of adsorbates is discussed. Three schemes, all extensions of the field emission current fluctuation method are presented and analyzed. The first consists of determining single site correlation functions with a STM in its more or less normal operating mode. The second consists of retracting the tip approximately one tip radius so that a circular region of high field is created on the flat surface from which field emission and diffusion induced current fluctuations can be obtained. The third considers creation of a

Block 20 Continued:

long narrow region of high field by placing a very fine cylindrical wire parallel to and above the plane substrate. This last scheme allows determination of diffusion anisotropy. Detailed expressions for the current correlation functions for the three schemes and criteria for allowed vibrational amplitudes and drift are derived. It is concluded that all three schemes should be feasible but probably would differ in the range of diffusion coefficient values they would be able to handle.

Extensions of the Field Emission Fluctuation Method for the Determination of Surface Diffusion Coefficients

Robert Gomer

Department of Chemistry
and James Franck Institute
University of Chicago
Chicago, Illinois 60637

ABSTRACT

The use of scanning tunneling microscopy and related techniques for the determination of surface diffusion coefficients of adsorbates is discussed. Three schemes, all extensions of the field emission current fluctuation method are presented and analyzed. The first consists of determining single site correlation functions with a STM in its more or less normal operating mode. The second consists of retracting the tip approximately one tip radius so that a circular region of high field is created on the flat surface from which field emission and diffusion induced current fluctuations can be obtained. The third considers creation of a long narrow region of high field by placing a very fine cylindrical wire parallel to and above the plane substrate. This last scheme allows determination of diffusion anisotropy. Detailed expressions for the current correlation functions for the three schemes and criteria for allowed vibrational amplitudes and drift are derived. It is concluded that all three schemes should be feasible but probably would differ in the range of diffusion coefficient values they would be able to handle.

85 9 09 061

Introduction

The field emission current fluctuation method for determining surface diffusion coefficients of adsorbates on metal surfaces, proposed by the author in 1973 [1,2] has been applied successfully to metals which can be fabricated into clean field emitters. It has recently been extended to measurements of diffusion anisotropy, i.e. a determination of the 2-dimensional diffusion tensors of adsorbates [3,4] and also provides the compressibility of the adlayer [5] and information on correlation lengths and their anisotropy [3,4]. A number of quite unexpected and interesting results have been obtained so far, which suggest that it would be worthwhile to extend the method to substrates which cannot easily be fashioned into clean field emitters. The recent advent of scanning tunneling microscopy (STM) [6] suggests some extensions of the method, which are outlined in this paper, together with calculations aimed at quantifying them. Finally some discussions of experimental constraints and feasibility criteria are given.

Single Site Correlation Function

The density-density time autocorrelation function evaluated at a single site provides essentially the same information as the "patch correlation function", used experimentally to date [1,2]. Monte Carlo simulations by Tringides and Gomer [7] use single site correlation functions extensively to obtain D. The function can be obtained in terms of t/τ_o where the relaxation time τ_o is here given by

$$\tau_o = a^2/4D \tag{1}$$

a is a dimension corresponding approximately to a substrate atomic radius. If the diffusion coefficient D is expressed as

$$D = \tfrac{1}{4}\, a^2 \nu e^{-E/kT} \tag{2}$$

it is seen from Eq. 1 that τ_o takes the particularly suggestive form

$$\tau_o = (\nu\, e^{-E/kT})^{-1} \qquad (3)$$

where ν is an effective attempt frequency and E the activation energy.

The smallness of τ_o for this case brings advantages and disadvantages. The main disadvantage is that a time τ_o should contain 100-200 individual correlation measurements or time boxes Δt so that $\Delta t \sim 0.01\ \tau_o$. This requires either that only small values of D be investigated or that rather fast electronics be employed. For instance if $D = 10^{-9}$ cm^2 sec^{-1} and $a^2 = 10^{-15}$ cm^2 $\tau_o = 2.5 \times 10^{-7}$sec, $\Delta t \sim 2.5$ nanosec. While this may be possible it would probably be necessary to work at temperatures so low that $D \leqslant 10^{-11}$ cm^2 sec^{-1} in order to increase τ_o and Δt accordingly. The advantage of small τ_o is that it may minimize drift and vibration problems, in that a single sequence of 200-400 channels containing one correlation measurement can be carried out over a given site without interference. Since the averaging required for a meaningful correlation function need not be restricted to the same site but can be carried out by summing measurements over equivalent sites slow lateral drift should be no problem. Vibrations which vary the tip-substrate spacing can also be removed in the single site mode, since it should be possible to clip the signal in order to make it uniform. All that is required is that the "occupied" signal differ sufficiently from the "empty" signal. In any case vibrational periods will generally be $\ll \tau_o$.

The mean square fluctuation is obtained as usual (2) as the zero time correlation function. To convert the observed value to a number fluctuation function it is only necessary to divide by the square of the amplitude corresponding to the "occupied" signal. It is perhaps worth pointing out that even at very low coverages where an ad-atom wanders into the field of view only occasionally the method gives the correct result, since the time averaging

involved in obtaining a correlation function automatically reduces its amplitude to the value corresponding to the particular coverage used. Ideally the latter should be determined independently. It may happen, however, that adsorbate coverage is very low, in which case at least an estimate may be obtained from f(o) since for very low coverages this quantity is equal to the mean particle number in the region of observation, i.e. directly gives the adatom to substrate atom ratio [5].

Patch and Line Correlation Functions

Although the single site method offers some attractive features it is limited to fairly low values of D as we have seen. Thus it is worthwhile to consider other, if related schemes. The following suggest themselves: (1) If a conventional field emitter is placed roughly one tip radius above a flat conducting surface, the field on the plane immediately under the emitter apex is quite high but falls off rapidly with the distance along the plane. Thus a relatively small area is "illuminated" and conventional field emission may be obtained from it. If the flat surface is covered with adsorbate which is mobile, a "conventional" field emission current fluctuation correlation function can be obtained. (2) If a sufficiently finely etched cylindrical wire is placed near and parallel to the surface a long rectangular region of high field will be created and diffusion across the narrow dimension can be observed as a one-dimensional correlation function [3]. If the wire is then rotated 90^{o} the other component of the diffusion tensor can be determined. These techniques differ from our present procedures only in that a flat substrate is the field emitter and a highly curved object serves to generate the requisite fields over relatively small areas. There is no insuperable problem, given the state of the STM art, in implementing the first scheme. It may be possible to implement the second by etching a very fine loop so

that its end approximates a flat cylinder, or by etching a blade-like emitter to simulate a short, thin half-cylinder. The main advantages of these schemes are that the states of the tip or cylindrical wire are relatively unimportant since they only serve to generate a field and to accept electrons. It will turn out, however, that the requirements on vibrational isolation and drift stability are still very severe and in particular require that the cylinder be short in length. We now discuss the forms of the current correlation functions f_i to be expected for these two configurations.

Tip Above a Plane

The envisaged geometry is shown in Fig. 1. For present purposes we assume that the tip can be replaced by a conducting sphere. The field at the plane surface is then given by

$$F(r)/F_o = (1 + (r/z_o)^2)^{-3/2} \tag{4}$$

z_o is the distance of the sphere's center from the surface, r is the radial distance along the surface from the origin shown in Fig. 1; F_o is the field on the surface at r = 0 and is given by

$$F_o = -V \frac{r_t(2z_o - r_t)}{z_o^2(z_o - r_t)} \tag{5}$$

where V is the applied voltage and r_t the tip radius. It is also useful to know the ratio of the plane surface to tip apex field:

$$F_{tip}/F_o = a^2 \frac{2a(a-1) + 1}{(2a-1)^2} \tag{6}$$

where $a = z_o/r_t$. If a = 2 this ratio is 2 so that the apex field will not be high enough to cause field desorption, field evaporation or field ionization if the field at the plane surface is 3-6 x 10^7 v/cm, i.e. typical for field emission.

We consider next the correlation function. Since relatively large areas of emission will be involved we work out only the analogue of $g_1(t)$ in Refs. 1 and 2. We then have from the Fowler-Nordheim equation

$$\ln j = \ln B - 6.8 \times 10^7 \, \phi^{3/2}/F \tag{7}$$

$$\begin{aligned} \delta \ln j &= c_1 \, \delta n + c_2 \, \delta\phi \\ &\tilde{=} (c_1 + 2\pi \, P c_2)\delta n \end{aligned} \tag{8}$$

where n is adsorbate density in atoms/cm^2,

$$c_1 = \frac{\partial \ln B}{\partial n} \tag{9}$$

$$c_2 = \frac{3}{2} \; 6.8 \times 10^7 \, \langle\phi\rangle^{\frac{1}{2}}/F \tag{10}$$

and

$$2\pi P = \frac{\partial \phi}{\partial n} \tag{11}$$

Here ϕ is work function, P adsorbate dipole moment, B a preexponential, and j current density. Since $\delta \ln j \tilde{\approx} \delta j/j$ we have from Eqs. 8 and 4

$$\begin{aligned} \langle \Delta i(o) \Delta i(t) \rangle &= \int_o^\infty d^2r \int_o^\infty d^2r' \; \bar{j}(r)\bar{j}(r') \; \langle \delta j(r,o) \; j(r',t) \\ &\tilde{=} (c_1 + 2\pi P c_2)^2 \langle j_o \rangle^2 \int_o^\infty d^2r \int_o^\infty d^2r' e^{-3/2 \, \alpha[(r/z_o)^2 + (r'/z_o)^2]} \langle \delta n(r,o) \; n(r',t) \rangle \end{aligned} \tag{12}$$

Here i is the emitted total current, Δi its fluctuation, $\bar{j}_o \equiv \langle j_o \rangle$ mean current density at r = 0 and

$$\alpha = 6.8 \times 10^7 \langle\phi\rangle^{3/2}/F_o \tag{13}$$

We have used the fact that $\bar{j}$ decreases very rapidly with decreasing F to expand F/F_o in Eq. 4. Since the term $\exp -\alpha(r/z_o)^2$ still falls off very rapidly with increasing r retaining the upper limit as ∞ in Eq. 12 introduces only a very small error. The quantity $\langle \delta n(r,o) \delta n(r',t) \rangle$ is

$$\langle \delta(r,o) \delta n(r',t) \rangle = \frac{S_o \, e^{-|r-r'|^2/4Dt}}{4\pi Dt} \tag{14}$$

where

$$S_o = \frac{\langle(\delta N)^2\rangle}{A} = k_B T K \langle n\rangle^2 \tag{15}$$

an intensive quantity [2,7]. Here $\langle(\delta N)^2\rangle$ is the total mean square number (not density) fluctuation in an area A and K the adlayer compressibility.

The total current $\langle i\rangle$ is found from

$$\langle i\rangle = 2\pi \int_o^\infty r dr \bar{j}_o \, e^{-\alpha(1+(r/z_o)^2)^{3/2}} \tag{16}$$

$$= \frac{2}{3\alpha} z_o^2 \pi \bar{j}_o$$

so that the current correlation function f_i

$$f_i(t) \equiv \frac{\langle \Delta i(o) \Delta i(t)\rangle}{\langle i\rangle^2} \tag{17}$$

is found from Eq. 11, after integration over the angle variables [1] to be

$$f_i(t) = \frac{S_o(c_1 + 2\pi P c_2)^2}{\pi z_o'^2 \tau} \int_o^\infty \rho d\rho \int_o^\infty \rho' d\rho I_o(2\rho\rho'/\tau) \, e^{-(1+\tau^{-1})(\rho^2+\rho'^2)} \tag{18}$$

Here

$$z_o' = \left(\frac{2}{3\alpha}\right)^{1/2} z_o \tag{19}$$

$$\rho = r/z_o' \tag{20}$$

$$\tau = t/\tau_o \tag{21}$$

$$\tau_o = z_o'^2/4D \tag{22}$$

I_o is the Bessel function J_o of imaginary argument. By further letting $\rho/\tau^{1/2} = x$ we have the integral

$$\tau \int_o^\infty x dx \int_o^\infty x' dx' I_o(2xx') e^{-(1+\tau)(x^2+x'^2)} \tag{23}$$

We multiply the integrand by $J_o(\gamma x')$ and let $\gamma \to 0$ after integration over x', which then yields, since $J_o(0) = 1$,

$$\lim_{\gamma \to 0} \int_o^\infty x' dx' \, e^{-\varepsilon x'^2} I_o(2xx') \, J_o(\gamma x') \tag{24}$$

$$= \lim_{\gamma \to 0} \frac{1}{2\epsilon} e^{\frac{4x'^2 - \gamma^2}{4\epsilon}} J_o\left(\frac{2x\gamma}{2\epsilon}\right)$$

$$= \frac{1}{2(1+\tau)} e^{\frac{x^2}{1+\tau}} \qquad (24)$$

where $\epsilon \equiv 1 + \tau$. Thus the integral over x becomes trivial and

$$f_i(t/\tau_o) = \frac{S_o(c_1 + 2\pi P c_2)^2}{\pi z_o'^2} \frac{1}{8 + 4(t/\tau_o)} \qquad (25)$$

A comparison of $f_i(t/\tau_o)$ according to Eq. 25 with $g_1(t/\tau_o)$ for a circular area of radius r_o is shown in Fig. 2. Clearly the functions are quite similar but not identical. It is interesting that the long time behavior of f_i is the expected one [2] namely

$$f_i(t) = \frac{S_o(c_1 + 2\pi P c_2)^2 4D}{\pi t} \qquad (26)$$

but that it does <u>not</u> contain z_o, so that in principle, D can be determined without knowing z_o.

<u>Cylinder Above A Plane</u>

It is assumed that the radius of the cylinder can be $r_o \sim 2\text{-}3 \times 10^{-5}$ cm so that its macroscopic length, which we will call 2b can be considered infinite, for purposes of estimating the field on the surface underneath the cylinder, even if $b = 10^{-3} - 10^{-4}$ cm. With this assumption the field on the surface at x = 0 (notation is shown in Fig. 3) is

$$F_o = -2V/[z_o \ln(2(z_o/r_o) - 1)] \qquad (27)$$

and the ratio

$$F(x)/F_o = (1 + (x/z_o)^2)^{-1} \qquad (28)$$

The ratio of the field at the cylinder surface (for x = 0) to that on the plane is

$$F_{cyl}/F_o = \frac{2}{a'(2-a')} \qquad (29)$$

where $a' = r_o/z_o$, r_o being the cylinder radius. If $a' = 0.5$ the field at the cylinder surface is 2.7 F_o so that again field desorption etc., will not take place. The total current field emitted from the substrate is

$$i = j_o \, 2b \, (\pi/\alpha)^{\frac{1}{2}} \, z_o \tag{30}$$

Here j_o is the current density corresponding to F_o and α is defined by Eq. 13.

If the cylinder is parallel to one of the principal axes of the diffusion tensor the density (and current) correlation function decomposes into a product of two 1-dimensional functions. We then have, by analogy to the previous development in this paper

$$f_i = \frac{S_o(c_1 + 2\pi P c_2)^2}{4b^2(\pi/\alpha) z_o^2} \int_{-\infty}^{\infty} dx \int_{-\infty}^{\infty} dx' e^{-\alpha[(x/z_o)^2 + (x'/z_o)^2]} \left(\frac{e^{-|x-x'|^2/4D_{xx}t}}{\sqrt{4\pi D_{xx} t}} \right) \int_{-b}^{b} dy \int_{-b}^{b} dy' \left(\frac{e^{-|y-y'|^2/4D_{yy}t}}{\sqrt{4\pi D_{yy} t}} \right) \tag{31}$$

The integrals over y, y' yield 2b since in the time of an experiment $f_y(t) \sim f_y(0)$ [3]. The quadratures over x, x' are elementary and one obtains finally

$$f_i(t) = \frac{S_o(c_1 + 2\pi P c_2)^2}{2b(\pi/\alpha)^{\frac{1}{2}} z_o} \quad \frac{1}{\sqrt{4\pi\tau + 2}} \tag{32}$$

where

$$\tau = t/\tau_o \tag{33}$$

and

$$\tau_o = \frac{z_o^2 \pi}{\alpha} \cdot \frac{1}{D_{xx}} \tag{34}$$

The form of f_i is compared with that for a rectangle in Fig. 4. It is apparent that the curves are remarkably similar. The long time behavior of f_i is given by

$$f_i(t) = \frac{S_o(c_1 + 2\pi P c_2)^2}{4b\,\pi^{\frac{1}{2}}} \quad \frac{1}{\sqrt{Dt}} \; ; \; \frac{t}{\tau_o} >> (1/2\pi) \tag{35}$$

which again, does not contain z_o. It is interesting to note that f_i is inversely proportional to 2b, the length of the cylinder. However, the actual current fluctuations, i.e. $\langle \Delta i(o) \Delta i(t) \rangle$ increase with b.

$$\langle \Delta i(o) \Delta i(t) \rangle = S_o (c_1 + 2\pi P c_2)^2 \langle j_o \rangle^2 (2\pi/\alpha)^{1/2} z_o b \qquad (36)$$

Thus an a.c. measurement, which is what is normally performed will actually yield a bigger signal the longer the cylinder, although stability considerations will show that b should be kept as small as possible.

Determination of α and z_o

The determination of activation energies requires only that z_o, the distance of the tip or cylindrical wire center from the plane substate be kept constant as the substrate temperature is varied. A determination of prefactors, i.e. absolute values of D requires, however, that α and z_o be known or at least approximated. We now indicate how this could be done:

(1) Tip above Plane

For this case the current emitted by the plane substrate is given by Eq. 16, which can be written, in view of the definition of α by Eq. 13, as

$$i = \frac{4\pi z_o^2}{3} \frac{Ck^3 V^3}{6.8 \times 10^7 \phi^{3/2}} e^{-6.8 \times 10^7 \phi^{3/2}/kV} \qquad (37)$$

where

$$k = F_o/V \qquad (38)$$

and C is the (image corrected) Fowler-Nordheim preexponential for a clean metal surface [8]

$$C = 6.2 \times 10^6 \frac{(\mu/\phi)^{1/2}}{\mu + \phi} e^{0.40\phi^{3/2}} \qquad (39)$$

The exponential term in the RHS of Eq. 39 comes about because the image correction term v(y) where

$$y = 3.8 \times 10^{-4} F_o^{1/2}/\phi \qquad (40)$$

which multiplies the Fowler-Nordheim exponent turns out to have the form

$$v(y) \tilde{=} 1 - 0.059 \times 10^{-7} F_o \tag{41}$$

so that the image correction appears as a factor in the Fowler-Nordheim preexponential.

It is therefore possible, at fixed z_o to determine $\ln i/V^3$ vs. $1/V$ (which is the analogue of a Fowler-Nordheim plot used in ordinary field emission) and from its slope to determine k, assuming that ϕ is known, for the clean surface. Thus α is found from Eqs. 13 and 38 for given V. z_o can then be found from the total current and Eqs. 37 and 39.

It is also possible to utilize Eq. 5 since

$$k = \frac{r_t(2z_o - r_t)}{z_o^2(z_o - r_t)} \tag{42}$$

if the emitter radius r_t is known, either from field emission measurements from the tip at large distance from the substrate or from independent determination. However, Eq. 5 is based on an assumed sphere-plane geometry and probably less accurate that the method described previously which uses only emission from the substrate.

(2) Cylinder Above Plane

For this case α and $k = F_o/V$ can be determined analogously to the tip-plane case by plotting $\ln i/V^{5/2}$ vs. $1/V$ as can be seen from Eq. 30. A procedure analogous to that outlined for the tip-plane case could then be used but turns out to be largely unnecessary since

$$k = \frac{2}{z_o} \cdot \frac{1}{\ln \; 2(z_o/r_o) - 1} \tag{43}$$

$$\tilde{=} \frac{2}{z_o}$$

since, for appreciable emission the logarithmic term is close to unity.

Stability Requirements

It is necessary also to examine the required stability of tip or cylinder both with respect to vibrations and "long-time" drift since small changes in tip-substrate or cylinder-substrate distance will lead to changes in fields and hence currents, which could interfere with the diffusion induced fluctuation signal.

(1) Tip Above Plane

(a) Vibrations

We ignore the effect of field on the preexponential term of the current and write, using Eqs. 7 and 16

$$\delta \ln i = \frac{\delta i}{i} = 6.8 \times 10^7 \, \phi^{3/2} \, \delta(1/F_o) = \alpha \frac{\delta F}{F} \tag{44}$$

Use of Eq. 5 then yields

$$\frac{\delta i}{i} = \alpha \, \delta a \left[\frac{2}{2a-1} - \frac{3a^2-1}{a^3-a} \right] \tag{45}$$

where $a \equiv z_o/r_t$, so that

$$\delta z_o = \left(\frac{\delta i}{i}\right) \cdot \left(\frac{r_t}{\alpha}\right) \left[\frac{2}{2a-1} - \frac{3a^2-1}{a^3-a} \right]^{-1} \tag{46}$$

We must now compare this signal with $\sqrt{f_i(o)}$ to get a sense of its importance. From Eq. 25 we have that

$$f_i(o) = \frac{\langle (\delta i)^2 \rangle}{\langle i \rangle^2} = \frac{\langle (\delta N)^2 \rangle}{A} \, \frac{(c_1 + 2\pi P c_2)^2}{8\pi \frac{2}{3\alpha} z_o^2} \tag{47}$$

We now assume roughly [7] that

$$\langle (\delta N)^2 \rangle \sim 0.1 \langle N \rangle = 0.1 \, A \langle n \rangle$$

so that

$$\sqrt{f_i(o)} = \left(\frac{0.1 \langle n \rangle (c_1 + 2\pi P c_2)^2}{8\pi \left(\frac{2}{3\alpha}\right)} \right)^{1/2} \frac{1}{a r_t} \tag{49}$$

where we have used $a \equiv z_o/r_t$.

We now require that

$$\left(\frac{\delta i}{i}\right)_{\text{vibration}} = \gamma \sqrt{f_i(o)} \tag{50}$$

where γ is a tolerance factor whose value depends on the details of the vibrational noise and the dynamic range of the correlator. If the noise is random and the dynamic range of the correlator sufficient $\gamma > 10\text{-}50$ might still allow extraction of a diffusion correlation function if the data collection time is increased accordingly. If vibrations are coherent γ might have to be as low as 0.1. Combining Eqs. 50, 49 and 46 we find assuming $a = 2$

$$\delta z_o = \gamma \frac{3}{7\sqrt{\alpha}} \left(\frac{0.3 \langle n \rangle}{8\pi}\right)^{\frac{1}{2}} (c_1 + 2\pi P c_2) \tag{51}$$

To get some feeling for numbers let us assume $\langle n \rangle \sim 10^{15}$ atoms/cm^2 and $\alpha = 20$ as before. We choose $c_1 \cong d\ln B/dn = -2\times10^{-15}$ cm^2/atom and $2\pi P = d\phi/dn = 1\times10^{-15}$ eV cm^2/atom; $c_2 = 10\,\phi^{\frac{1}{2}}/F$ if F is expressed in volts/Å; we let $c_2 = 7.5\ (\text{eV})^{-1}$ corresponding to $\phi = 5$ eV and $F = 0.3$ volt/Å. These values correspond approximately to oxygen on a W(110) plane [9]. We then find that $\delta z_o = \gamma\ 0.2$ Å. If $\gamma \geq 1$ is tolerable the vibrational amplitude is within the limits of STM technology. It is interesting, incidentally, that δz_o is independent of z_o (or r_t) and depends only on the ratio $\underline{a}$, although not dramatically. This relative independence of δz_o on collector radius suggests a way of circumventing vibrational noise which generally is of low frequency. If the collector is made fairly sharp and or if the measurements are carried out at high enough temperature to make τ_o so small that the relevant frequency domain lies outside that of the mechanical vibrations γ could be much larger than suggested above.

(b) Drift

In addition to vibrations one might also be faced with a more or less

steady drift. We will assume that $\beta\tau_o$ is the minimum collection time, i.e. that β runs of duration τ_o each must be taken to obtain a meaningful average. β is probably $\geqslant 10^3$ depending on random noise. We will also assume that in time $\beta\ \tau_o$ the mean value of the emission current must change by $\leqslant 0.1 \langle i \rangle$. We then have, combining Eqs. 45 and 22 and assuming a = 2, that

$$\frac{dz_o}{dt} \leqslant \frac{0.13\ D}{\pi\ \beta\ r_t} \tag{52}$$

If r_t = 300 Å, D = 10^{-11} $cm^2 sec^{-1}$ and $\beta = 10^3$ we find dz_o/dt = 0.01 Å/sec. While this seems very stringent it should be remembered that it is possible to regulate z_o at rates (i.e. frequencies) which do not interfere with the correlation signal by adjusting the servomechanism to hold the mean current fixed, even though the a.c. component is being used to obtain a correlation signal.

(2) Cylinder Above Plane

(a) Vibrations

For this case one finds from Eqs. 7 and 27 that

$$\delta i/i = \alpha\ dz_o/z_o \tag{53}$$

since the change in the logarithmic term in Eq. 27 can be ignored. An analysis similar to that leading to Eq. 51 then gives

$$\delta z_o = 4.4\text{x}\ 10^{-9}\ \gamma(z_o/b)^{\frac{1}{2}} \tag{54}$$

assuming the same numerical values of α, $\langle n \rangle$, c_1, and $2\pi P$ used previously. If γ = 10 we find that δz_o = 1.42 Å if z_o/b = 0.1 and 0.45 Å if z_o/b = 0.01; if z_o = 4000 Å b could therefore be as much as $4\text{x}10^{-3}$ cm and still give a tolerable value of δz_o. However, for cylindrical geometry τ_o is necessarily larger than for the hemispherical collector, since we have assumed that the cylinder radius is larger. Thus the domain of frequencies of relevance to the correlation function will be lower and may include vibrational frequencies, so that γ may have to be < 10, the value assumed here.

Nevertheless, there should be some ranges of D which can be investigated with the cylindrical collector, at least as far as vibration amplitudes are concerned.

(b) Drift

We use Eq. 34 for τ_o and find

$$dz_o/dt \leq \frac{0.1\ D_{xx}}{\beta \pi z_o} \tag{55}$$

If we assume z_o = 4000 Å and $\beta = 10^3$ we find $dz_o/dt \leq 8 \times 10^7 D$ Å/sec. This very low value puts a rather definite limit on measurable D values, i.e. > 10^{-9} $cm^2 sec^{-1}$, but this is consistent with the fact that τ_o is larger than for the hemispherical collector.

Field Effects

We consider finally the effect of high field, not on diffusion per se but on the changed adsorbate concentration arising from field-dipole and polarization effects. In a region of high field the adsorbate density is

$$n(f) = n(0)\ \exp(\tfrac{1}{2}\ \alpha\ F^2/kT + P.F/kT) \tag{56}$$

where n(F) and n(0) are the adsorbate densities in the field and field free regions respectively; α is the polarizability and P the dipole moment. If the field is appropriate for field emission and the negative end of the dipole moment points outward, i.e. if the work function is raised by adsorption P.F in Eq. 56 is positive; if there is a work function decrease caused by adsorption P.F in Eq. 56 is negative. For P in Debye, α in $Å^3$ and F in volts/Å Eq. 56 takes the form

$$n(f) = n(0)\ \exp[(403\ \alpha F^2 + 2.42 \times 10^3\ P.F)/T] \tag{57}$$

For α = 1 $Å^3$, P = 0.27 Debye (corresponding to $\Delta\phi$ = 1 eV for n = 10^{15} atoms/cm^2) and F = 0.4 volts/Å we find, at 300 K n(f)/n(0) = 2.96 and 1.7 at 600 K This is a substantial

increase and indicates that the concentration in the probed region may be considerably enhanced. This is no fundamental obstacle since the concentration in the probed region can be measured by determining the work function change.

Diffusion itself will also be affected in two ways. First D is generally a function of n and thus having different values of n in the probed region and beyond may affect measurements. Second, roughly speaking atoms now undergo biassed random walks since there is a field contribution on to their binding energy. Nevertheless, the situation is not as bad as it might appear, for roughly the same reason why field variation is not a serious problem in the fluctuation method employing a field emitter as substrate: In that case the field also drops off as one moves away from the tip apex but the region over which diffusion is of importance is confined to that region of the tip where the field is nearly uniform. In the present case field emission is a much more sensitive function of F and hence r than the contribution of F to binding energy; in particular we have picked a rather high polarizability in the example and in most cases of interest $\frac{1}{2}\alpha F^2$ can probably be neglected, so that only the P.F term remains. Then field emission occurs from a relatively small region of almost uniform F while diffusion will occur with nearly constant D from a much larger region with nearly constant n. It is easy to show, for the tip above plane case, from Eqs. 4 and 57 for the values of α, P and F used that n/n(0) will have decreased from 2.96 at $(r/z_o)^2 = 0$ to 2.27, i.e. by only 30% at $(r/z_o')^2 = 5$, which corresponds to 2.24 times the radius of the probed region. Nevertheless, the field effect cannot be neglected and must be considered case by case. For the single site method where very small fields can in principle be used it can probably be neglected altogether. It should perhaps be pointed out that the effect we are considering here

is different from that of a uniform high field everywhere on the activation energy of diffusion. This latter effect concerns the differences in P, F and $\frac{1}{2} F^2$ at the potential minima and saddle points of diffusing atoms and is important only for high dipole moments and very high polarizabilities, such as are encountered for adsorbed alkali atoms.

Conclusion

The foregoing has indicated that it may be possible to measure surface diffusion coefficients of adsorbates by extensions of the field emission current fluctuation correlation method. Three possible schemes have been proposed and analyzed. Each is most suitable for a different range of diffusion coefficients, since the relaxation times involved are different. Each method has somewhat different constraints imposed by vibrational noise and drift. In general vibrational noise and drift within a given scheme are antagonistic: In order to overcome vibrational noise longer data collection times will be required and this requires less drift or better drift compensation. However, it appears that each method could actually be used over a limited range of D values.

No attention has been paid to actual design considerations, i.e. the need to prepare clean substrates, maintain ultrahigh vacuum and control coverage, for instance by work function measurements, or how to achieve temperature variation without appreciably changing the collector-substrate distance. These problems, although not trivial, seem soluble. For instance, emission from the collector can always be used to control its distance from the substrate, even when the latter is a semiconductor with temperature dependent field emission. Thus there is some hope that the schemes proposed here can actually be implemented.

Acknowledgments

This work was supported in part by ONR Contract N00014-77-C-0018. I have also benefitted from the Materials Research Laboratory of the National Science Foundation at the University of Chicago. Finally it is a pleasure to thank IBM Europe and in particular Dr. H. Rohrer for giving me the opportunity to participate in the IBM Workshop on Scanning Tunneling Microscopy, Oberlech, Austria, July, 1985, which provided a concrete feeling for the potentialities and also difficulties inherent in STM.

References

[1] R. Gomer, Surf. Sci. 38, 373 (1973).

[2] G. Mazenko, J. R. Banavar, and R. Gomer, Surf. Sci. 107, 459 (1981).

[3] D. R. Bowman, R. Gomer, K. Muttalib and M. Tringides, Surf. Sci. 138, 581 (1984).

[4] M. Tringides and R. Gomer, Surf. Sci. 155, 254 (1985).

[5] B. Bell, R. Gomer, and H. Reiss, Surf. Sci. 55, 494 (1976).

[6] G. Binnig, H. Rohrer, Ch. Gerber, and E. Weibel, Phys. Rev. Lett. 49, 57 (1982).

[7] M. Tringides and R. Gomer, Surf. Sci. 145, 121 (1984).

[8] R. Gomer, Adv. in Chem. Phys. 27, 211 (1974).

[9] J.-R. Chen and R. Gomer, Surf. Sci. 79, 413 (1979).

Figure Captions

1) Schematic diagram of tip-plane geometry: r_t radius of (assumed spherical) tip; r vector in the surface from origin directly under the tip apex in the plane; z_o distance from emitter center to surface.

2) Comparison of correlation function $g_1(t/\tau_o)$ for a circular aperature of radius r_o, for which $\tau_o = r_o^2/4D$ (solid line and scale marked (a)) with normalized correlation function $f_i = 2/(2 + t/\tau_o)$ for the tip-above plane geometry (points and scale marked (b)). For this latter case $\tau_o = (2/3\alpha)z_o^2/4D$ and the horizontal axis has been displaced for best fit with the $g_1(t/\tau_o)$ curve.

3) Schematic diagram of the cylinder-plane geometry: r_o, cylinder radius; z_o, distance from cylinder axis to surface; x-y, coordinate frame in the surface plane; 2b, length of cylinder.

4) Comparison of 1-dimensional correlation function for the side of a rectangle of width 2a (solid line and scale marked (a)) for which $\tau_o = a^2/D_{xx}$ with normalized correlation function $[2/(2 + 4\pi t/\tau_o)]^{\frac{1}{2}}$ (points and scale marked (b)), for which $\tau_o = \pi z_o^2/\alpha D_{xx}$. The horizontal axis has been displaced for best fit of points to line.

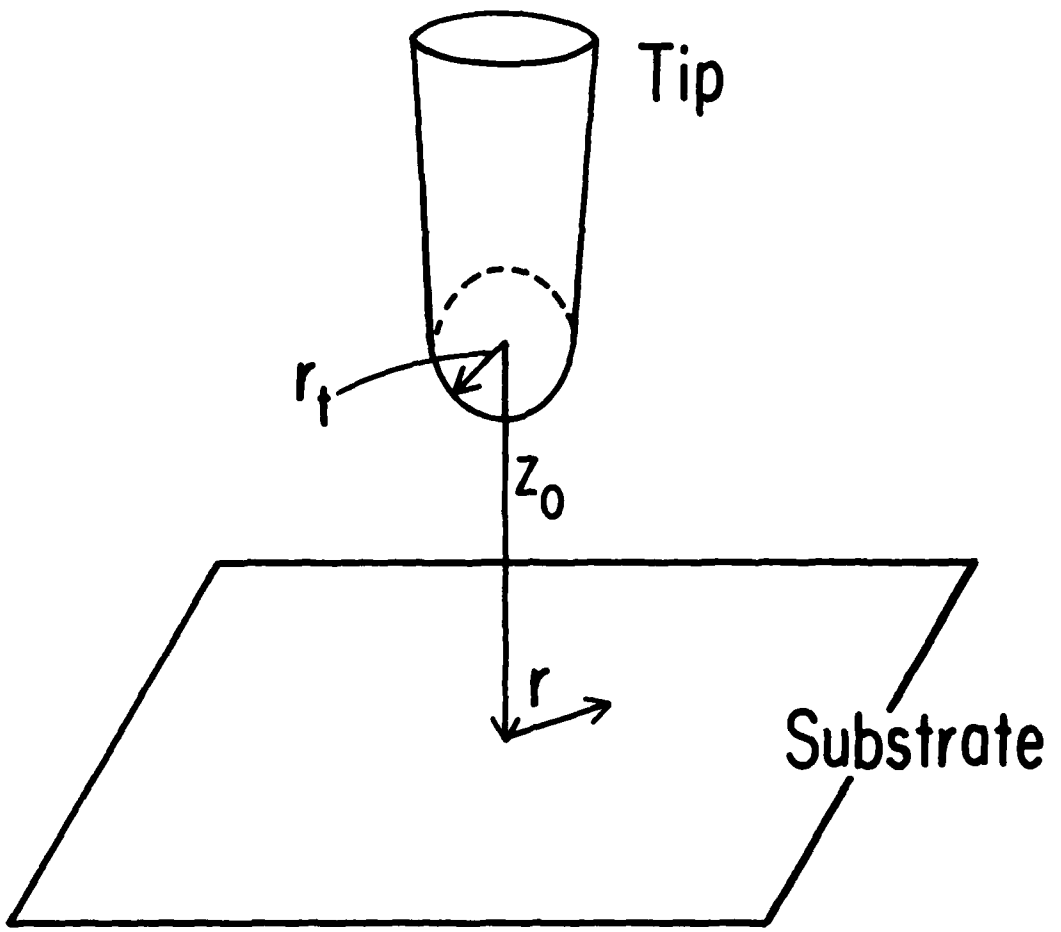

Fig.1

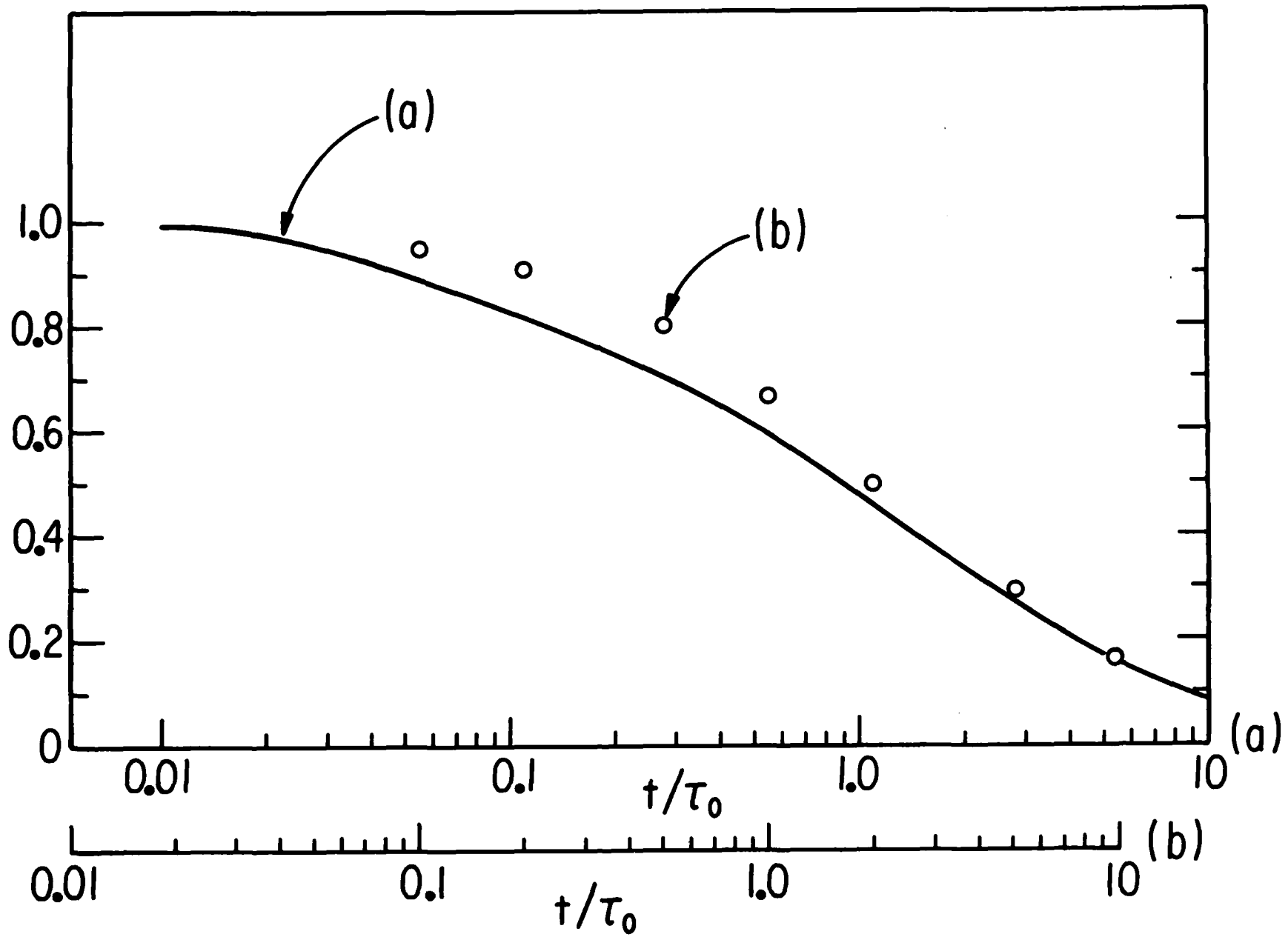

Fig.2

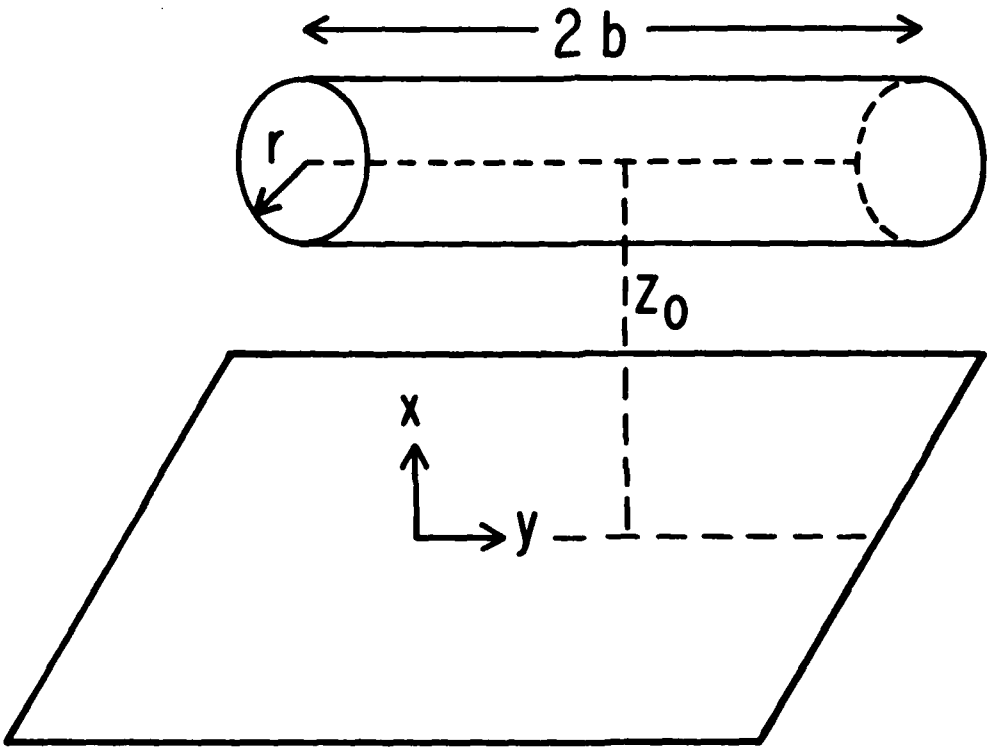

Fig.3

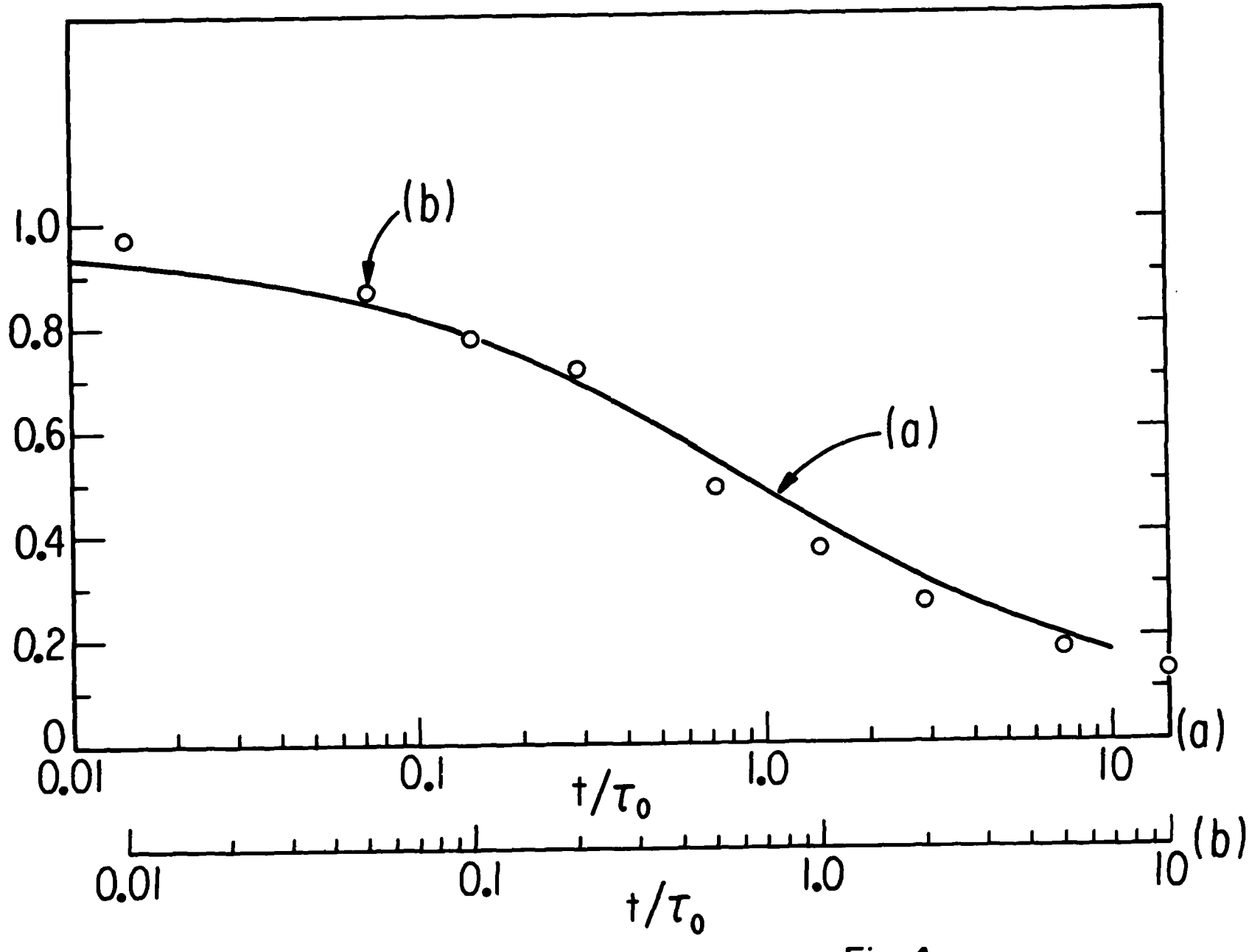

Fig.4

END

FILMED

11-85

DTIC